Journal of Medicinal Chemistry

pubs.acs.org/jmc

Article

First-in-Class Allosteric Inhibitors of DNMT3A Disrupt Protein−Protein Interactions and Induce Acute Myeloid Leukemia Cell Differentiation

Jonathan E. Sandoval, Raghav Ramabadran, Nathaniel Stillson, Letitia Sarah, Danica Galonić Fujimori, Margaret A. Goodell, and Norbert Reich*

Cite This: *J. Med. Chem.* 2022, 65, 10554−10566

Read Online

ACCESS | Metrics & More | Article Recommendations | Supporting Information

ABSTRACT: We previously identified two structurally related pyrazolone (compound 1) and pyridazine (compound 2) allosteric inhibitors of DNMT3A through screening of a small chemical library. Here, we show that these compounds bind and disrupt protein−protein interactions (PPIs) at the DNMT3A tetramer interface. This disruption is observed with distinct partner proteins and occurs even when the complexes are acting on DNA, which better reflects the cellular context. Compound 2 induces differentiation of distinct myeloid leukemia cell lines including cells with mutated DNMT3A R882. To date, small molecules targeting DNMT3A are limited to competitive inhibitors of AdoMet or DNA and display extreme toxicity. Our work is the first to identify small molecules with a mechanism of inhibition involving the disruption of PPIs with DNMT3A. Ongoing optimization of compounds 1 and 2 provides a promising basis to induce myeloid differentiation and treatment of diseases that display aberrant PPIs with DNMT3A, such as acute myeloid leukemia.

INTRODUCTION

The epigenetic machinery regulates a wide range of biological processes including parental imprinting, cellular development, and differentiation.[1−4] Epigenetic regulation is a highly dynamic process that is achieved by the action and modulation of writers (DNMTs, HATs, and HMTs) that catalyze the addition of specific modifications on DNA or histone tails, erasers that remove specific marks, or readers that are recruited to specific modifications.[5,6] Given the reversibility of epigenetic modifications, interest in the development of therapeutics targeting epigenetic enzymes has increased in recent years, especially allosteric modulators.[7,8] While some success has been realized for some epigenetic enzymes, such as histone modifiers, others have proven challenging in this regard.[9−12] For instance, the FDA-approved nucleoside inhibitors (azacytidine and decitabine), which function as prodrugs that are incorporated into DNA to inhibit the human DNA methyltransferases, are highly cytotoxic due to the formation of irreversible suicide complexes.[13−15] In addition to these competitive inhibitors of DNMTs, several molecules that act as cofactor S-adenosyl-L-methionine (AdoMet) competitors to inhibit DNMT3A and other DNMTs have been described.[16−20] However, the use of competitive inhibitors of DNMTs presents several disadvantages compared to allosteric inhibitors in terms of specificity within a family of related proteins, nonrelated proteins with shared cofactors, or inability to target surfaces involved with modulation of enzymatic activity. A recent report on a first-in-class reversible DNMT1-selective inhibitor showed promising in vivo results.[21] The inhibitor acts by an intercalation mechanism, which may have off-target consequences. Our focus on DNMT3A is motivated by its frequent mutation in multiple cancers including various forms of leukemia and its limited expression within a subset of stem cells and tumors.[22,23]

Epigenetic mechanisms are characterized by highly integrated pathways involving extensive crosstalk mediated by protein−protein interactions (PPIs).[24−26] For instance, DNMT3A interacts with the polycomb repressive complexes 2 (PRC2), a multimeric complex associated with transcriptional silencing that is composed of various histone modifiers and long noncoding RNAs.[27−32] Through this interaction, DNMT3A-mediated DNA methylation contributes to the silencing of PRC2 target genes.[27−29] Therefore, the disruption of protein−protein complexes could be a route to develop highly specific drugs targeting epigenetic pathways. The development of small molecules targeting PPIs has proven more challenging compared to molecules targeting active sites due to the unique physicochemical properties of surfaces

Received: May 9, 2022
Published: July 22, 2022

https://doi.org/10.1021/acs.jmedchem.2c00725
J. Med. Chem. 2022, 65, 10554−10566

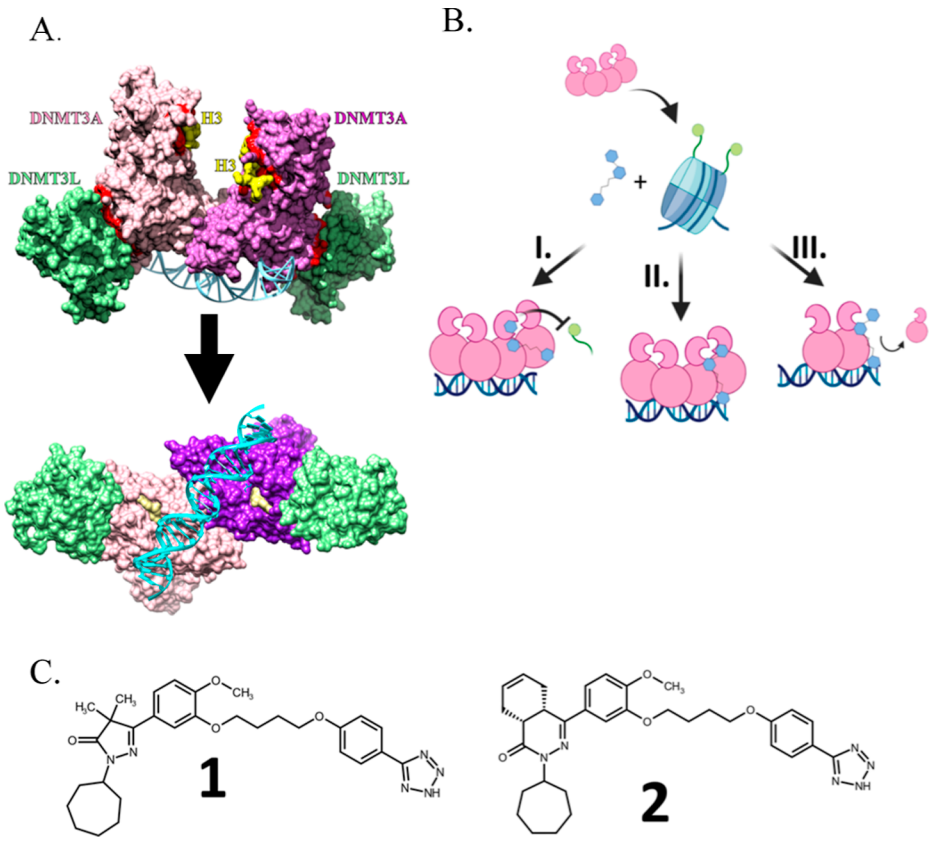

Figure 1. Surfaces involved with allosteric modulation of DNMT3A and models for disruption of modulation by compounds 1 and 2. (A) Front and bottom view of a DNMT3A heterotetramer (pink ■ and violet ■; a.a. 468−912) in complex with DNMT3L (green ■; a.a. 171−379) and histone H3 peptides (yellow ■; 1−12) with surfaces involved with interactions (red ■; <5 Å) (adapted from PDB 4U7T). DNA (blue ■) was modeled using the structure of a DNA-bound DNMT3A-DNMT3L complex (PDB 5YX2). (B) Upon binding a target nucleosome, compounds 1 or 2 may disrupt the allosteric modulation of DNMT3A by H3 tails (I.) or PPIs at the tetramer interface (II and III). (C) Structure of related pyrazolone (1) and pyridazine (2) inhibitors.

involved with PPIs.[33−35] However, recent successes have identified small-molecule inhibitors of epigenetic PPIs, specifically in distinct types of histone reader proteins and scaffolding proteins of epigenetic complexes.[33−35] In addition to being recurrently mutated in patients with acute myeloid leukemia (AML), the biological importance of DNMT3A is highlighted by the fact that DNMT3A interacts with a wide range of proteins with distinct biological functions, some of which share a binding surface with DNMT3L (Figure 1A).[22,23,36−39] Thus, DNMT3A is a suitable target for the potential use of small molecules to target PPIs in diseases such as AML.

Recent work from our lab identified two compounds that do not display a competitive mechanism with DNA or AdoMet, and inhibition of enzymatic activity is due to binding an allosteric region outside the active site (Figure 1A,C).[40] Given that the ATRX-DNMT3-DNMT3L (ADD) domain or the tetramer interface of DNMT3A presents two well-characterized surfaces for allosteric modulation of enzymatic activity (Figure 1A, we assessed whether compounds 1 or 2 disrupt interactions at these surfaces (Figure 1B).[41,42] With the use of mutational mapping and radiochemical and binding assays under various conditions, we show that compounds 1 or 2 selectively inhibit DNMT3A activity by disrupting interactions at the tetramer interface and that this mechanism of inhibition persists even when DNMT3A is in complex with distinct partner proteins. This work presents the characterization of two novel compounds with the potential use for modulation of epigenetic pathways through disruption of PPIs, which are likely to not display the toxicity commonly observed with current therapeutics targeting DNMT3A.[13−15]

RESULTS

Compounds 1 and 2 disrupt DNMT3A_WT homo- or heterotetramers but not interactions with histone H3 tails.

While there have been several efforts to develop small-molecule inhibitors of DNMTs, to date, the FDA has only approved two nucleoside inhibitors (azacytidine and decitabine), which are highly cytotoxic.[13,15] We recently reported the discovery of two compounds (Figure 1C) that act as allosteric inhibitors of DNMT3A (i.e., not competitive with S-adenosylmethionine or DNA).[40] However, the precise mechanism of action (Figure 1B) or the surface on DNMT3A bound by these inhibitors remains unknown (Figure 1A). Histone H3 tails and DNMT3L act as allosteric activators of DNMT3A activity by binding the ADD domain or the tetramer interface of DNMT3A, respectively.[41,42] Therefore, we assessed whether the allosteric inhibitors (compound 1 or 2) disrupt the modulation of DNMT3A activity by histone H3 tails or DNMT3L (Figure 2). We observed that when DNMT3A_WT was preincubated with DNMT3L and compound 1 (navy blue ■ Figure 2B) or 2 (navy blue ■, red−blue ■ Figure 2B), the activity of DNMT3A_WT is lower compared to similar reactions with DNMT3A_WT

https://doi.org/10.1021/acs.jmedchem.2c00725
J. Med. Chem. 2022, 65, 10554−10566

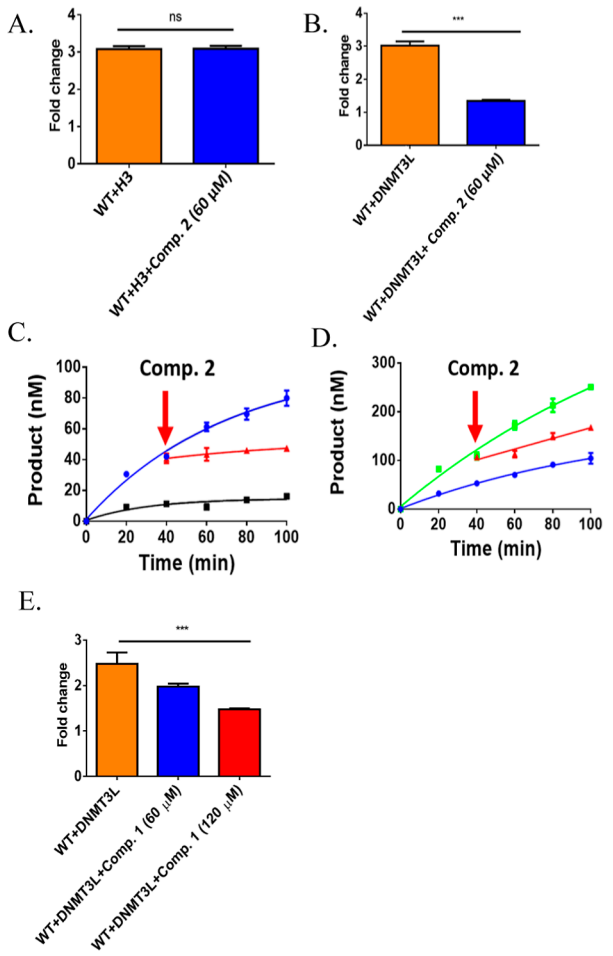

Figure 2. Compounds 1 and 2 do not inhibit the activation of DNMT3A_WT by H3 peptides but disrupt DNMT3A-DNMT3L interactions at the DNMT3A tetramer interface. While compound 2 fails to disrupt the activation of full-length DNMT3A_WT by H3 peptides (**A**), compounds 1 and 2 inhibit the stimulation of DNMT3A_WT activity by DNMT3L in reactions at equilibrium (B,E.) and actively methylate DNMT3A_WT homotetramers (red ■ (C); navy blue ■ DNMT3A_WT, ■ DNMT3A_WT with compound 2) or DNMT3A_WT−DNMT3L heterotetramers (red ■ (D); navy blue ■ DNMT3A_WT, green ■ DNMT3A_WT−DNMT3L). Reactions in (A,B,E) consisted of 150 nM DNMT3A_WT preincubated for 1 h at 37 °C with H3 peptides (5 μM; residues 1−21) (**A**) or DNMT3L [150 nM; (B,E)] in buffer containing compound 1 (E) or 2 (A,B). While reactions in (C,D) consisted of 50 nM DNMT3A_WT, reactions in (D) consisted of DNMT3A_WT−DNMT3L (1:1 at 50 nM) that was preincubated for 1 h at 37 °C prior to the start of the reaction. All reactions (A−E) were initiated by the addition of poly dI-dC (5 μM). Fold change (A−E) refers to the data normalized to the activity of reactions consisting of DNMT3A_WT only. All data reflect the mean and s.d. of three independent experiments. A *T*-test (A,B) or one-way analysis of variance (E) was used to compare the values of reactions containing compound 1 (E) or 2 (A,B) to those without compound 1 or 2 (ns, $p > 0.05$; ***, $p < 0.001$).

incubated with DNMT3L (navy blue ■ Figure 2B,E; ***, $p < 0.001$). In contrast, similar experiments with the activating H3 peptide (navy blue ■ Figure 2A) show that compound 2 does not alter DNMT3A_WT activity (orange ■ Figure 2A) in the presence of the H3 peptide (navy blue ■ Figure 2A) (orange ■ Figure 2A; ns, $p > 0.05$.).[41] Although DNMT3A and histone-modifying enzymes, such as lysine-specific demethylase 5A (KDM5A), are structurally unrelated and modify distinct components of nucleosomes, both epigenetic enzymes act on nucleosome substrates and are readers and writers of specific epigenetic modifications.[43] We sought to determine whether compounds 1 and 2 affect the activity of KDM5A to assess the specificity of these compounds for DNMT3A over an unrelated epigenetic enzyme. We found that compounds 1 and 2 minimally affect the demethylase activity of KDM5A relative to CPI-455, a well-established KDM5 inhibitor (Figure S2).[44] Based on the inhibition of DNMT3L-mediated stimulation of DNMT3A_WT activity by compound 1 or 2 in reactions at equilibrium (Figure 2B,E), we tested whether compound 2 disrupts DNMT3A_WT homo- or heterotetramers by carrying out DNA methylation (Figure 2C,D). The addition of compound 2 decreases the activity of DNMT3A_WT homotetramers (red ■ Figure 2C) or DNMT3A_WT−DNMT3L heterotetramers (red ■ Figure 2D) relative to similar reactions in which dimethyl sulfoxide (DMSO) was added to catalytically active DNMT3A_WT homotetramers (navy blue ■ Figure 2C) or DNMT3A_WT−DNMT3L heterotetramers (green ■ Figure 2D). Thus, compound 2 disrupts interactions at the tetramer interface of DNMT3A in actively catalyzing protein complexes, which better models the cellular dynamics between DNMT3A, DNA, and distinct partner proteins.

In addition to DNMT3L, the activity of DNMT3A is modulated by distinct partner proteins through direct interactions with the tetramer interface of DNMT3A[22,23,36−39] (Figure 1A). Given that compounds 1 and 2 disrupt the activation of DNMT3A activity by DNMT3L (Figure 2), we monitored the oligomeric state of DNMT3A_WT homo- or heterotetramers in the presence of these compounds (Figure 1B, II. or III). For this approach, we measured the fluorescence anisotropy of a fluorescein (5′/6-FAM)-labeled 27-mer (GCbox30 duplex) in complex with DNMT3A_WT homo- or heterotetramers in the presence of compounds 1 and 2 (Figure 3).[45,46] We relied on the use of p53 or TDG to explore the effects of compound 1 or 2 on DNMT3A_WT heterotetramers, given that the interactions between DNMT3A and p53 or TDG have been previously characterized and are implicated in AML.[36,37,45] We found that the addition of compound 1 (red ■ Figure 3A) or 2 (red ■ Figure 3B) decreases the fluorescence anisotropy of DNA-bound DNMT3A_WT homotetramers compared to similar reactions with DMSO (■ Figure 3A,B). Furthermore, increasing the concentrations of DNMT3A_WT results in a lower change in the initial fluorescence anisotropy of FAM-DNA in reaction with compound 1 (red ■ Figure 3C) or 2 (red ■ Figure 3D) relative to those with DMSO (■ Figure 3C,D). Similarly, increasing concentrations of compound 1 (navy blue ■ Figure 3E,F) or 2 (red ■ Figure 3E,F) drastically decreases the initial fluorescence anisotropy of DNMT3A_WT-p53 (Figure 3E) or DNMT3A_WT-TDG (Figure 3F) heterotetramers bound to FAM-DNA compared to similar reactions consisting of DNMT3A_WT homotetramers (green ■ Figure 3E,F) or heterotetramers with p53 (■ Figure 3E) or TDG (■ Figure 3F) challenged by the addition of DMSO. In fact, we observed that increasing levels of compound 1 (navy blue ■ Figure 3E,F) or 2 (red ■ Figure 3E,F) to DNMT3A_WT-p53 (Figure 3E) or DNMT3A_WT-TDG (Figure 3F) heterotetramers on FAM-DNA led to a final anisotropy value comparable to reactions with DNMT3A_WT dimers and compound 2 (600 μM) at the start of the reaction

https://doi.org/10.1021/acs.jmedchem.2c00725
J. Med. Chem. 2022, 65, 10554−10566

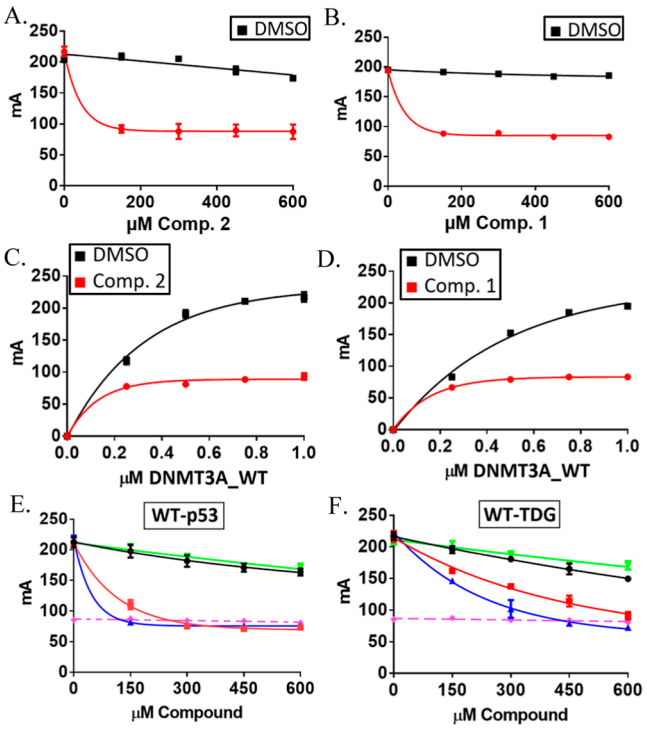

Figure 3. Compounds 1 and 2 disrupt DNA-bound DNMT3A_WT in complex with distinct partner proteins. While the addition of DMSO (A,B) does not disrupt DNA-bound (50 nM 5′ FAM-6-labeled GCbox30 duplex) DNMT3A_WT homotetramers (1 μM), increasing concentrations of compound 1 (B) or 2 (A) decrease the fluorescence anisotropy (millianisotropy units (mA)) of DNMT3A_WT complexes on DNA. The addition of DNMT3A_WT to reactions consisting of compound 1 (D) or 2 (C) leads to a lower change in the fluorescence anisotropy of FAM-labeled substrate DNA relative to similar reactions with DMSO (C,D). Increasing concentrations of compound 1 (navy blue ■ E,F) or 2 (red ■ E,F) decrease the fluorescence anisotropy of DNMT3A_WT-p53 (E) or DNMT3A_WT-TDG (F) complexes on DNA (GCbox30 duplex). The following reactions were performed as controls in (E,F): DNMT3A_WT with DMSO [green ■; (E,F)], DNMT3A_WT-p53 with DMSO (■ E), DNMT3A_WT-TDG with DMSO (■ F) and DNMT3A_WT with compound 2 at the beginning of the reaction [pink ■; (E,F)]. Data reflect the mean and s.d. of three independent experiments.

(pink ■ Figure 3E,F). In sum, our observation that the addition of compounds 1 and 2 under distinct conditions decreases the background-subtracted (FAM-DNA only) initial fluorescence anisotropy of DNMT3A_WT homotetramers−FAM-DNA complexes (Figure 3) is consistent with the inhibition of enzymatic activity by these compounds involving disruptions of the oligomeric state of DNMT3A (Figure 1B III).

Oligomerization of DNMT3A_ R771A with DNMT3L Restores Inhibition by Compound 2. In previous work, we show that substitutions to specific residues at the tetramer interface of DNMT3A disrupt the oligomeric state, processive catalysis, and modulation by partner proteins.[45−48] Given that compounds 1 and 2 disrupt interactions between DNMT3A_WT and distinct partner proteins that bind the tetramer interface (Figures 2 and 3), we carried out molecular docking and dynamics simulations to predict critical residues for interactions with compounds 1 or 2 and assess the stability of these interactions in silico (Figure S3).[45−48] This approach has been previously carried out for other human DNMTs and was validated by docking the S-adenosyl-L-homocysteine (SAH) ligand into the active-site pocket to within 2.0 A of its crystal structure pose (submitted for publication).[42,49−51] Following docking of compounds 1 or 2 to the tetramer interface of DNMT3A monomers (Figure S3A,C), the root-mean-squared deviation (rmsd) for each compound with respect to the protein backbone during a 10 ns simulation was plotted (Figure S3D). As indicated by the change in the rmsd values for compounds 1 or 2 over the course of the simulation (Figure S3D), our in silico analysis shows that these compounds adopt a stable conformation on the tetramer interface of DNMT3A. Interestingly, calculations of the free energy and energetic contributions of the individual residues to the interaction between the DNMT3A tetramer interface and compounds 1 or 2 identified several key residues for oligomerization and PPIs as the largest contributors to this interaction [molecular mechanics (MM)/GBSA calculations; see the Experimental Section; Figure S3A,C].[45−48] Based on these observations and data showing that compounds 1 and 2 interfere with interactions at the tetramer interface of DNMT3A (Figures 1B and 2), we assessed the effect of compound 2 on the DNMT3A tetramer interface alanine substitutions (R729, E733, R736, and R771; Figure S1).

Initially, we assessed the effect of compound 1 or 2 on the activity of DNMT3A tetramer interface mutants in reactions initiated by the addition of substrate DNA following a short preincubation (10 min) with compound 2 (Figure 4A,B). While all the DNMT3A tetramer interface mutants (R729, E733, R736, and R771) displayed reduced inhibition to compound 2 relative to DNMT3A_WT (Figure 4A; ***, $p < 0.001$), we found that DNMT3A_R771A (red ■ Figure 4B) was the only mutant that was not inhibited by compound 2 (ns, $p > 0.05$; *, $p < 0.01$). We then carried out similar reactions consisting of DNMT3A tetramer interface mutants that were preincubated with DNMT3L and compound 2 prior to being initiated (Figure 4C,D). We found that in these reactions, inhibition of DNMT3A tetramer interface mutants (R729, E733, R736, and R771) in complex with DNMT3L was comparable to that observed for DNMT3A_WT−DNMT3L heterotetramers (Figure 4C; ns, $p > 0.05$), unlike reactions without DNMT3L where inhibition by compound 2 was reduced (Figure 4A,B). Furthermore, compound 2 inhibited the activity of DNMT3A_R771A in DNMT3A_R771A-DNMT3L heterotetramers (red ■ Figure 4D), which was not observed in reactions without DNMT3L (red ■ Figure 4B). To further examine the inhibition of DNMT3L-mediated activation of DNMT3A tetramer interface mutants (red ■ Figure 4D), we then assessed the effect of compound 2 on the fluorescence anisotropy of tetramer interface mutant DNMT3A-DNMT3L heterotetramers bound to FAM-DNA (Figure 4E). We initially monitored changes in the fluorescence anisotropy of dimeric DNMT3A tetramer interface mutants bound to FAM-DNA by the addition of DNMT3L to confirm the formation of tetramer interface mutant DNMT3A−DNMT3L heterotetramers. The increase in the fluorescence anisotropy of FAM-DNA bound by DNMT3A_R771A (red ■ Figure 4E) or DNMT3A_R729A (navy blue ■ Figure 4E) observed by the addition of DNMT3L was comparable to the fluorescence anisotropy values of DNMT3A_WT−DNMT3L heterotetramers in complex with FAM-DNA (■ Figure 4E). While the addition of DMSO did not alter the fluorescence anisotropy of these

https://doi.org/10.1021/acs.jmedchem.2c00725
J. Med. Chem. 2022, 65, 10554−10566

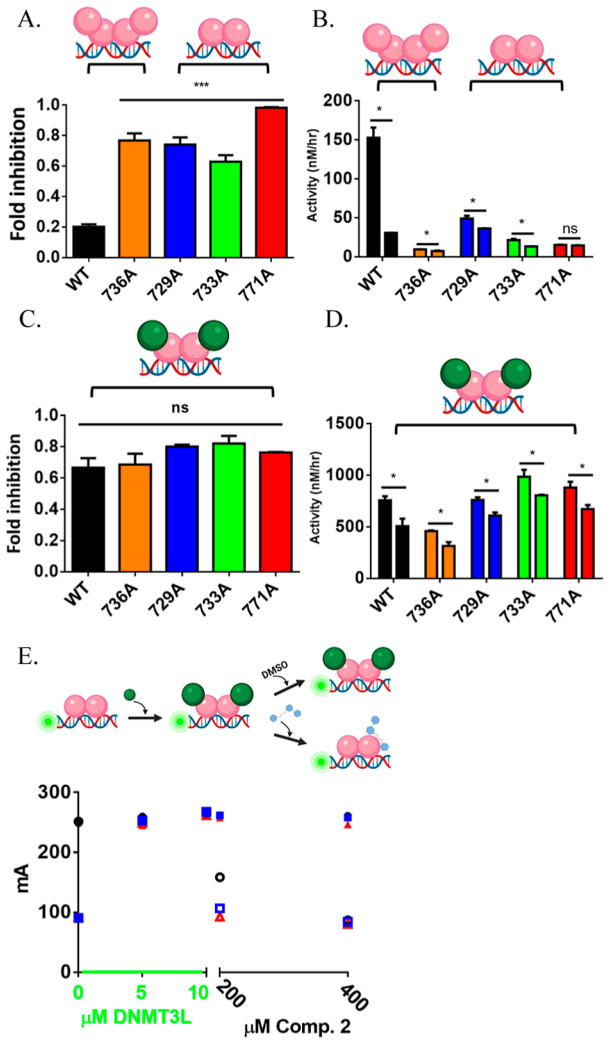

Figure 4. Compound 2 inhibits DNMT3A_ R771A-DNMT3L heterotetramers but not DNMT3A_ R771A homodimers. (A,B.) DNMT3A tetramer interface mutants are differentially responsive to modulation by compound 2 relative to WT with R771A unresponsive to inhibition (B). (C,D.) Formation of mutant DNMT3A heterotetramers with DNMT3L leads to comparable levels of inhibition by compound 2 as WT−DNMT3L complexes and restores inhibition of R771A (D). (E) The addition of compound 2 decreases the fluorescence anisotropy of DNMT3L heterotetramers with DNMT3A WT (■), R771A (red □), or R729A (navy blue □) bound to FAM-labeled DNA (GCbox30 duplex). Similar reactions consisting of DNMT3L in complex with DNMT3A WT (■), R771A (red ■), or R729A (navy blue ■) to which DMSO was added were performed as controls. (A−D) consisted of 150 nM WT or mutant DNMT3A, 150 nM DNMT3L (C,D.; preincubated for 1 h at 37 °C) and were initiated by the addition of poly dI-dC (5 μM). In (C,D), fold inhibition was calculated as follows: 1—(product formed with compound 2/product formed without compound 2). A one-way analysis of variance (A,C) was used to compare the values of reactions with DNMT3A mutants to those with WT. A *T*-test (B,D) was performed to compare the values of reactions containing compound 2 to those without compound 2 (ns, $p > 0.05$; ***, $p < 0.001$; *, $p < 0.01$). All data reflect the mean and s.d. of three independent experiments. Compounds 1 and 2 disrupt interactions at the tetramer interface of DNMT3A_R882H.

complexes (Figure 4E, DNMT3L with ■ DNMT3A_WT, red ■ DNMT3A_R771A or navy blue ■ DNMT3A_R729A), the addition of compound 2 reduced the fluorescence anisotropy of FAM-DNA bound by DNMT3A_WT (□; Figure 4E), DNMT3A_R771A (red □; Figure 4E), or DNMT3A_R729A (navy blue □ Figure 4E) in complex with DNMT3L to comparable levels as that observed prior to the addition of DNMT3L. Therefore, our data show that the formation of DNMT3A_R771A-DNMT3L heterotetramers restores the ability of compound 2 to inhibit DNMT3A_R771A activity by disrupting interactions at the tetramer interface (Figure 1B).

The DNMT3A R882H-substitution is the most frequently detected *DNMT3A* mutation in AML patients.[22,23,39] Although located at the DNA binding surface of DNMT3A (Figure S1), the R882H-substitution appears to alter the interactions between DNMT3A and distinct partner proteins, including those that bind the DNMT3A tetramer interface.[45,52,53] Given the biological impact of R882H substitutions and the effect of R882H on PPIs involving DNMT3A, we explored the consequences of compounds 1 or 2 on DNMT3A_R882H-DNMT3L heterotetramers (Figure 5). Like that observed in reactions with DNMT3A_WT (Figure 2B), we found that a 1 hour preincubation of DNMT3A_R882H, DNMT3L, and compound 1 (navy blue ■, red ■ Figure 5B) or 2 (navy blue ■, red ■ Figure 5A) decreases the activation of DNMT3A_R882H by DNMT3L relative to similar reactions consisting of DNMT3A_R882H, DNMT3L, and DMSO (red

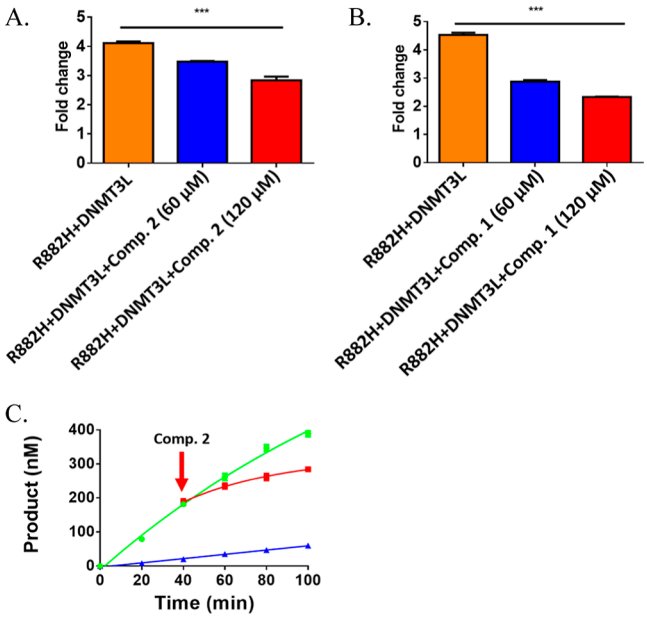

Figure 5. Compounds 1 and 2 inhibit the activation of DNMT3A_R882H by DNMT3L. (A,B) Compounds 1 and 2 disrupt the activation of DNMT3A_R882H enzymatic activity by DNMT3L in reactions at equilibrium (A,B), as well as actively methylating DNMT3A_R882H-DNMT3L complexes [red ■ (C)]. Reactions in (A,B) consisted of 150 nM DNMT3A_R882H preincubated for 1 h at 37 °C with DNMT3L (150 nM; B,E) in buffer containing compound 1 (E) or 2 (A,B). Reactions in (C) consisted of 50 nM DNMT3A_R882H (navy blue ■) and DNMT3A_R882H-DNMT3L (green ■; 1:1 at 50 nM and preincubated for 1 h at 37 °C). All reactions (A−C) were initiated by the addition of poly dI-dC (5 μM). Fold change (A,B) refers to data normalized to the activity of reactions consisting of DNMT3A_R882H only. A one-way analysis of variance (A,B) was carried out to compare the averages of reactions with DNMT3A_R882H−DNMT3L complexes under various conditions.

https://doi.org/10.1021/acs.jmedchem.2c00725
J. Med. Chem. 2022, 65, 10554−10566

■ Figure 5A,B; ***, $p < 0.001$). Furthermore, the addition of compound 2 (yellow ■ Figure 5C; 120 μM) decreases product formation (nM methylated DNA) in catalytically active DNMT3A_R882H-DNMT3L heterotetramers relative to reactions with DNMT3A_R882H-DNMT3L heterotetramers challenged with the addition of DMSO (green ■ Figure 5C). Therefore, our data are consistent with compounds 1 and 2, disrupting the interactions between DNMT3A_R882H and DNMT3L at the tetramer interface of DNMT3A_R882H, including catalytically active protein complexes.

To further examine the effect of compounds 1 or 2 on PPIs involving DNMT3A_R882H, we monitored the fluorescence anisotropy of DNA-bound DNMT3A_R882H in complex with distinct partner proteins and under various conditions (Figure 6). As observed in tetramer interface mutants (R729A and R771A, Figure 4 E), the addition of DNMT3L increases the initial fluorescence anisotropy of DNMT3A_R882H dimers on FAM-DNA (red ■, ■ Figure 6A,B). Compared to reactions with DNMT3A_R882H-DNMT3L heterotetramers to which DMSO was added (■ Figure 6A,B), the addition of compound 1 (red ■ Figure 6B) or 2 (red ■ Figure 6A) reduces the fluorescence anisotropy of DNA-bound DNMT3A_R882H-DNMT3L to similar levels as that observed prior to the addition of DNMT3L. Moreover, the addition of DNMT3L does not appear to change the initial fluorescence anisotropy of DNMT3A_R882H complexes on FAM-DNA in reactions with compound 1 (red ■ Figure 6D) or 2 (red ■ Figure 6C) compared to similar reactions with DMSO (■ Figure 6C,D). To assess whether this effect (Figure 6A–D) is also observed in DNMT3A_R882H heterotetramers, we monitored the fluorescence anisotropy of DNA-bound DNMT3A_R882H in complex with p53 (Figure 6E) or TDG (Figure 6F) challenged with increasing concentrations of compound 1 or 2. P53 or TDG were used for these assays as their interactions with DNMT3A have been previously characterized.[36,37,45] The addition of DMSO minimally reduces the fluorescence anisotropy of DNA-bound DNMT3A_R882H heterotetramers with DNMT3L (green ■ Figure 6E,F), p53 (■ Figure 6E), or TDG (■ Figure 6F). However, increasing concentrations of compound 1 (navy blue ■, Figure 6E,F) or 2 (red ■, Figure 6E,F) decreased the fluorescence anisotropy of DNA-bound DNMT3A_R882H-p53 (E) or DNMT3A_R882H-TDG (F) heterotetramers to similar levels as that observed in reactions consisting of DNMT3A_R882H, DNMT3L and compound 2 from the start of the reaction (pink ■, Figure 6E,F). Here, we show that compounds 1 and 2 disrupt PPIs involving the biomedically relevant R882H-substitution in DNMT3A and partner proteins with distinct biological functions.

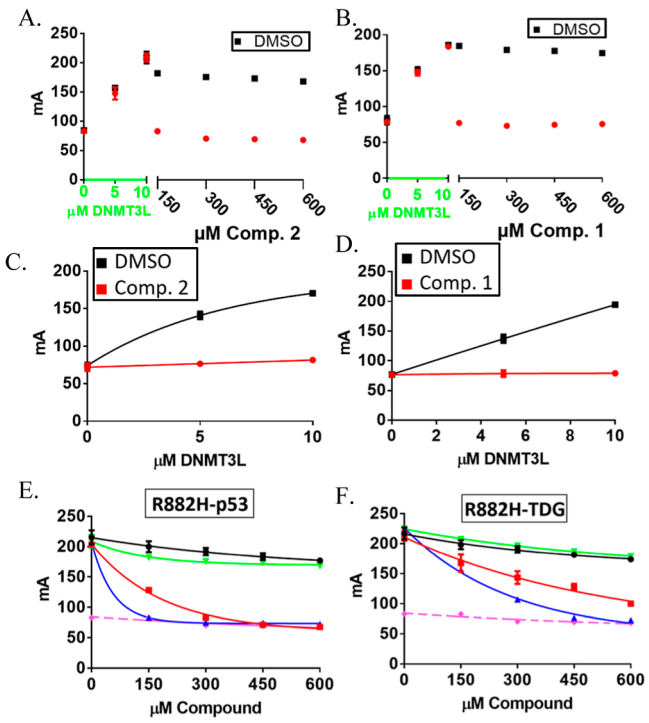

Figure 6. Compounds disrupt DNMT3A_R882H heterotetramers with distinct partner proteins. The addition of compound 1 (B) or 2 (A) decreases the fluorescence anisotropy (millianisotropy units (mA)) of DNA-bound (50 nM 5′ FAM-6-labeled GCbox30 duplex) DNMT3A_R882H–DNMT3L complexes relative to similar reactions to which DMSO was added (A,B). While the addition of DNMT3L increases the fluorescence anisotropy of DNMT3A_R882H in complex with DNA in DMSO (C,D), increasing levels of DNMT3L do not change the fluorescence anisotropy of DNA-bound (GCbox30 duplex) DNMT3A_R882H in the presence of compound 1 (D) or 2 (C). Increasing amounts of compound 1 (navy blue ■; E,F) or 2 (red ■; E,F) decrease the fluorescence anisotropy of DNMT3A_R882H-p53 (E) or DNMT3A_R882H-TDG (F) complexes on DNA (GCbox30 duplex). (E,F.) The following reactions were performed as controls: DNMT3A_R882H–DNMT3L with DMSO (green ■; E,F), DNMT3A_R882H-p53 (■; E), or -TDG (■; F) with DMSO and DNMT3A_R882H–DNMT3L with compound 2 at the beginning of the reaction (pink ■; E,F). All data reflect the mean and s.d. of three independent experiments. Compound 2 induces myeloid differentiation and decreases global levels of 5-methylcytosine in distinct AML cell lines.

Given the novel mechanism of inhibition by compound 2 as a disrupter of PPIs with DNMT3A, we sought to investigate the antileukemic potential of compound 2 by assessing apoptosis and differentiation in a panel of human AML cell lines after treatment with compound 2. Cell viability assays, using annexin V staining to detect apoptotic cells, performed following a 72 h treatment of compound 2 showed a dose–response effect with a marked increase in apoptosis in the 7–12 μM range (Figure S5). The resulting IC_{50} values for the AML cell lines assessed (Figure S5) are comparable to what has been reported for azacytidine under similar experimental conditions.[54−56] CD11b, an integrin family member responsible for leukocyte adhesion and migration during an inflammatory response, is often used as a marker of myeloid differentiation and to detect the therapeutic potential of modulators of DNMTs.[57−61] Therefore, we then monitored CD11b levels in live cells to determine whether modulation of DNMT3A by compound 2 impacted the differentiation status of leukemia cells. For this, AML cell lines were stained with markers for CD11b and propidium iodide (PI) following a 72 h treatment of DMSO or increasing concentrations of compound 2, and CD11b levels were monitored in PI negative cells only (Figures 7 and S4). Relative to DMSO-treated cell populations, we observed that compound 2 led to a concentration-dependent increase in the myeloid differentiation marker, CD11b, in multiple PI-negative AML cell lines: MV411 (biphenotypic B myelomonocytic leukemia), MOLM13 (acute monocytic leukemia), THP-1 (acute monocytic leukemia), OCI-AML3 (DNMT3A R882 mutant, AML), KASUMI (acute myeloblastic leukemia), HL60 (acute

https://doi.org/10.1021/acs.jmedchem.2c00725
J. Med. Chem. 2022, 65, 10554−10566

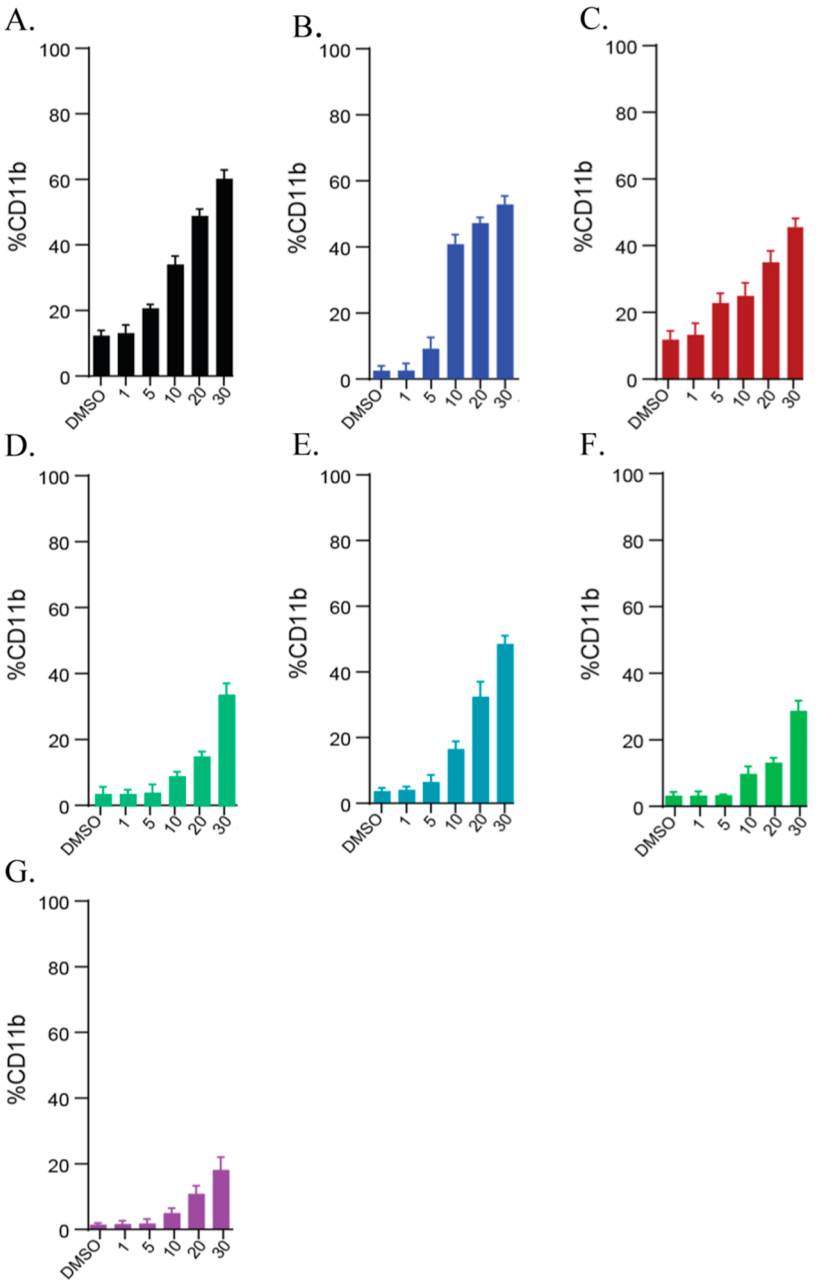

Figure 7. Compound 2 induces expression of the CD11b differentiation marker in a panel of distinct live AML cell lines in a concentration-dependent manner. Increasing concentrations of compound 2 increased CD11b expression in (A) MV411 (■), (B) MOLM13 (teal blue ■), (C) THP1 (dark red ■), (D) OCI-AML3 (green ■), (E) KASUMI (blue ■), (F) HL60 (green ■), and (G) K562 (violet ■) cell populations. Histograms in (A–G) display the changes in the percentage of CD11b positive cells as evaluated by flow cytometric analysis (Figure S4). Cells were harvested and stained with markers for CD11b following a 72 h treatment of DMSO or varying concentrations of compound 2. Data reflect the mean and s.d. of three independent experiments.

promyelocytic leukemia), and K562 (chronic myelogenous leukemia) (Figures 7 and S4).

DNA methylation plays a critical role in leukemogenesis. Decreases in cellular DNA methylation levels result from treatment with demethylating agents such as azacytidine and decitabine, resulting in AML transformation by promoting differentiation.[62−65] Since DNMT3A inhibition by compound 2 may likely result in changes in DNA methylation, we used an ELISA to assay for changes in global DNA methylation (Figure 8). We observed that a 5 μM treatment of compound 2 led to a time-dependent decrease in DNA methylation across three leukemia cell lines (HL60, OCI-AML3, and K562). Importantly, changes in DNA methylation occur concomitantly with our observations of increased differentiation after 3 days at a lower concentration of compound 2 (Figure 8). Here, we show that compound 2 achieves similar phenotypic outputs, like differentiation and apoptosis, as the FDA-approved nucleoside inhibitors. However, modulation of DNMT3A by compound 2 presents an improvement in these nucleoside inhibitors due to the distinct mechanism of inhibition and capacity for the generation of analogues with improved features.[66]

https://doi.org/10.1021/acs.jmedchem.2c00725
J. Med. Chem. 2022, 65, 10554−10566

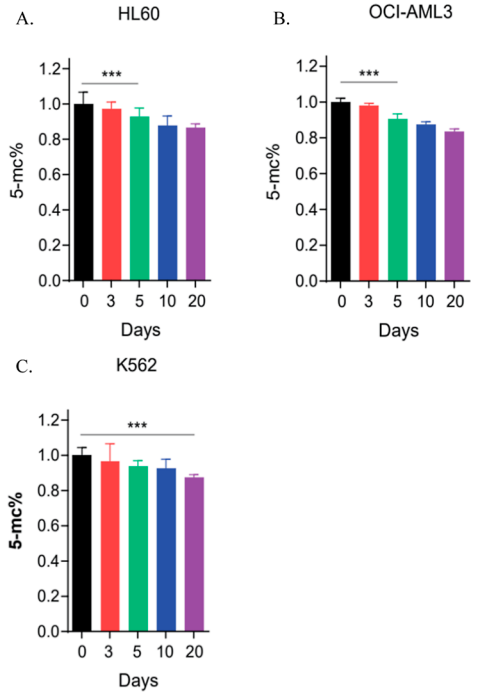

Figure 8. Compound 2 leads to a time-dependent decrease of global 5-methylcytosine. Global genomic DNA methylation was measured in a panel of AML cell lines [(A) HL60, (B) OCI-AML3, and (C) K562] on indicated days after the addition of 5 μM compound 2 (antibody detection by ELISA). Data reflect the percentage of 5-methylcytosine (5-mc %) and changes to 5-mc % over the course of the experiment were compared to day 0. Data reflect the mean and s.d. of three independent experiments.

DISCUSSION AND CONCLUSIONS

There is expanding experimental evidence that epigenetic mechanisms are interdependent and comprise a regulatory network, whose crosstalk contributes to transcriptional regulation.[24−26] Given that this crosstalk involves the interactions of distinct multimeric protein complexes, therapeutics targeting PPIs of epigenetic writers, readers, and erasers are of keen interest.[35] Small-molecule therapeutics targeting DNMTs are limited to nucleoside inhibitors (azacytidine and decitabine) and molecules that act as competitive inhibitors of substrate DNA or cofactor AdoMet, which have been reported as being cytotoxic.[13−21] These observations led us to screen a diverse chemical library in which we identified two structurally related pyrazolone (compound 1) and pyridazine (compound 2) allosteric inhibitors of DNMT3A.[40] Here, we present evidence that inhibition of enzymatic activity by compound 1 or 2 is achieved through disruption of PPIs at the tetramer interface of DNMT3A in DNMT3A homo- or heterotetramers (Figure 1B). Compounds 1 and 2 are the only reported small-molecule inhibitors of PPIs with DNMT3A to date. Therefore, our findings present the potential use of these compounds to chemically manipulate the modulation of DNMT3A and the treatment of malignancies associated with aberrant modulation of DNMT3A activity, such as AML.[22,23,39,45,47,48]

Previously, we reported two allosteric inhibitors that inhibit enzymatic activity by binding outside the active site (Figure 1A). Subsequently, we assessed whether compounds 1 and 2 disrupt interactions at the allosteric surfaces known to modulate DNMT3A (red ■, Figure 1A) to help define their mechanism of action. Given that compounds 1 and 2 disrupt interactions at the tetramer interface of DNMT3A (Figure 2B−E), but not at the ADD domain (Figure 2A), our data are consistent with these compounds acting as inhibitors of PPIs without impacting DNMT3A-H3 tail interactions (Figure 1B II,III). Furthermore, we show that this inhibition of PPIs persists in catalytically active DNMT3A_WT homo- or heterotetramers (Figure 2C,D), as well as DNMT3A_R882H heterotetramers (Figure 5C), which better models the cellular interactions of DNMT3A and highlights the therapeutic potential of these compounds. Our anisotropy results show that the addition of compounds 1 or 2 results in the formation of a smaller DNMT3A_WT−FAM-DNA complex, suggesting that both compounds disrupt interactions between DNMT3A and partner proteins (Figure 1B III). Furthermore, this mechanism of action is not specific to WT DNMT3A−DNMT3A interactions at the tetramer interface as we obtained similar results for two partner proteins with a shared binding surface on DNMT3A but are associated with distinct biological functions (Figure 3E,F).[36,37,45,48] The direct association and functional cooperation between DNMT3A and partner proteins with distinct biological functions is well documented.[27−29,36,37,45,48] In fact, it has been shown that DNMT3A may act as a scaffold for epigenetic regulatory complexes in addition to directly influencing the activity of distinct partner proteins.[27−29,36,37] Thus, the use of small molecules targeting binding partners of DNMT3A, like compounds 1 and 2, may serve to manipulate the DNA methylation-independent activities of DNMT3A.

Specific residues at the dimer (R882) and tetramer interface (R729, E733, R736, and R771) of DNMT3A are often mutated in AML patients and have been identified as major contributors to the oligomeric state, processive catalysis, and modulation by partner proteins.[22,39,45,47,48] We show that compounds 1 and 2 inhibit the activity of homodimer mutants (R729A, E733A, and R882H) located at both the dimer (R882H, Figure 5A−C) and tetramer (R729A and E733A, Figure 4A,B) interfaces (Figure S1). Thus, inhibition of DNMT3A activity by compounds 1 and 2 does not come entirely from disruptions of PPIs at the tetramer interface, and once bound, these compounds further inhibit the catalytic activity of DNMT3A (Figure 1BIII). We also identified a dimer mutant located at the tetramer interface (R771A) (Figure S1) that was only responsive to inhibition of enzymatic activity (Figure 4A−D) through disruption of PPIs by compound 2 in heterotetrameric complexes with DNMT3L (Figure 4E). The molecular dynamics simulations suggest that compounds 1 and 2 stably bind the tetramer interface (Figure S3) and provide insights into the amino acid residues responsible for binding compounds 1 or 2. Thus, our work could serve as a guide for future structure−activity relationship (SAR) studies for the development of more efficacious analogues of compounds 1 and 2. Mutation of DNMT3A (R882H) contributes to leukemogenesis by silencing differentiation-associated genes in hematopoietic stem cells (HSCs) in a DNA methylation-independent manner through the aberrant recruitment of the PRC1 complex.[52] Here, we show that compounds 1 and 2 disrupt the activation of DNMT3A R882H through PPIs at the tetramer interface (Figure 5A−C), and perhaps, more notably, these compounds disrupt DNMT3A R882H complexes with distinct partner proteins (Figure 6A−F). Given that the R882H substitutions impact distal interactions at the tetramer interface (Figure S1), future

https://doi.org/10.1021/acs.jmedchem.2c00725
J. Med. Chem. 2022, 65, 10554−10566

SAR studies starting from compounds 1 and 2 may additionally lead to the development of small molecules that specifically target DNMT3A R882H and the aberrant PPIs associated with this substitution, like that observed with PRC1 in leukemogenesis.[45,47]

Apoptosis and differentiation of human AML cell lines are routinely assessed to determine the antileukemic potential of novel demethylating agents.[67−69] Based on our findings that compound 2 allosterically inhibits DNMT3A activity by disrupting PPIs (Figures 2 and 3), we assessed the ability of compound 2 to induce apoptosis and differentiation in a panel of distinct human AML cell lines. Using cell-based assays, previous studies report IC50 values for azacytidine in the concentration range of 12−20 μM. We found that compound 2 led to a dose-dependent increase in apoptosis with an IC50 in the 7−12 μM range for the cell lines assessed, which is comparable to that observed for azacytidine (Figure S5). Interestingly, we also observed a dose-dependent increase of CD11b in live AML cell lines, which robustly increases above 5 μM (Figure 7). Taken together, our results suggest that the increase in apoptosis likely comes from the loss of self-renewal due to the increase in differentiation. Furthermore, we found that the ability of compound 2 to induce apoptosis and differentiation was comparable in cell lines carrying wild-type DNMT3A alleles (MV411, MOLM13, KASUMI, HL60, K562, and THP1) or with an R882 substitution (OCI-AML3). These findings are in line with our enzymatic studies showing comparable responsiveness to compound 2 in reactions with WT (Figures 2 and 3) or R882H (Figures 5 and 6) DNMT3A. The complex network and crosstalk between distinct epigenetic mechanisms contribute to HSC differentiation.[70] In fact, the interplay between DNA methylation and histone modifications appears to largely contribute to the differentiation and regulation of HSCs.[70] DNMT3A directly interacts with distinct histone modifiers, including components of the PRC2 repressive complex.[27−29] Given that compound 2 disrupts PPIs with DNMT3A, future studies could evaluate the impact of compound 2 on the DNA methylation-independent activities of DNMT3A including changes to histone modifications. Here, we present evidence that compound 2 leads to similar phenotypic outputs as the FDA-approved nucleoside inhibitors. However, given the distinct mechanisms of action (formation of a suicide complex compared to inhibition of PPIs), it is likely that the pathway to these outputs differs between compound 2 and nucleoside analogues. Furthermore, the mechanism of action by compound 2 is more suitable for improvement, unlike nucleoside analogues.

In summary, our study characterized the inhibition of DNMT3A activity by the recently described compounds 1 and 2 and revealed that the mechanism of inhibition involves disruption of PPIs at the tetramer interface. The ability to allosterically manipulate the DNA methylation activity and interactions involving DNMT3A provide a basis for improved toxicity, which is dose-limiting for currently used drugs targeting DNA methylation.[13−20] Further optimization of these compounds and the discovery of novel PPI inhibitors provide a promising approach for the treatment of diseases that cause disruption of the PPIs associated with DNMT3A, such as AML.[52,53]

EXPERIMENTAL SECTION

Purity Statement. All the compounds used in our study were >95% pure, as determined by high-performance liquid chromatography (HPLC) analysis (Figure S6).

Expression Constructs. The plasmids used for the expression of recombinant human proteins were as follows: pET28a-hDNMT3A-Copt for DNMT3A full length,[71] pET28a-hDNMT3A_catalytic_domain for wild-type or mutants of the DNMT3A catalytic domain (Δ1−633),[72] pTYB1-3L was used to express full-length human DNMT3L,[38] pET15b-human p53 for the expression of full-length (1−393) human p53[73] and pET28a-hTDG for full-length TDG (1−410).[74] DNMT3A mutants were generated using pET28a-hDNMT3A_catalytic_domain as a template and are described in ref 47.

Protein Expression and Purification. DNMT3A full-length and catalytic domain (WT and mutants), DNMT3L, p53, and TDG were expressed in NiCo21(DE3) competent *Escherichia coli* cells (New England Biolabs). Cells were grown in the Luria−Bertani medium at 37 °C to an A600 nm of 0.9 (DNMT3A full length), 0.7 (DNMT3A catalytic domain WT and mutants), 0.7 (DNMT3L), 0.6 (p53), and 0.8 (TDG). Protein expression was induced by the addition of 1 mM isopropyl-β-D-thiogalactopyranoside (GoldBio) after lowering the temperature to 28 °C. The induction times were 5 h for DNMT3A full-length and catalytic domain (WT and mutants), 5 h for DNMT3L, 5 h for TDG, and 16 h for p53. Cell pellets were harvested by centrifugation at 5000*g* for 15 min and stored at −80 °C.

DNA Methylation Assays. DNA methylation reactions were carried out to monitor the ability of DNMT3A to incorporate tritiated methyl groups from AdoMet onto DNA substrates in the absence or presence of compounds 1 and 2 under distinct experimental conditions involving biological modulators of DNMT3A (histone tails and partner proteins). Assays were performed at 37 °C in a methylation reaction buffer consisting of 50 mM KH_2PO_4/K_2HPO_4 (pH 7.8), 1 mM ethylenediaminetetraacetic acid (EDTA), 1 mM dithiothreitol (DTT), 0.2 mg/mL bovine serum albumin (BSA), 20 mM NaCl, and with saturating AdoMet (15 μM). For these reactions, 50 μM ([^{3}H] methyl-labeled: unlabeled, 1:10) AdoMet stocks were prepared from 32 mM unlabeled AdoMet (NEB) and [^{3}H] methyl-labeled AdoMet (80 Ci/mmol; supplied by PerkinElmer) in 10 mM H_2SO_4. Poly dI-dC (5 μM) was used as a substrate due to the increased activity of DNMT3A in this substrate, which allows a higher level of detection of changes in enzymatic activity. Reactions were quenched by mixing aliquots taken from a larger reaction with 0.1% sodium dodecyl sulfate (1:1) and spotted onto Hybond-XL membranes (GE Healthcare). Samples were then washed, dried, and counted using a Beckman LS 6000 liquid scintillation Counter as described in ref 75. In reactions assessing the disruption of PPIs with DNMT3A at equilibrium, DNMT3A was incubated for 1 h at 37 °C in methylation reaction buffer containing compounds 1, 2, or DMSO prior to initiating the reaction by the addition of poly dI-dC.

KDM5A Enzymatic Assays. Time-resolved fluorescence resonance energy transfer (TR-FRET) assays were carried out using $KDM5A_{1-797}$ enzymes in 384-well white opaque OptiPlate (PerkinElmer). Half-log serial dilutions of CPI-455 (Axon MedChem), compound 1 and compound 2 in DMSO were added to the assay buffer [50 mM N-(2-hydroxyethyl)piperazine-N′-ethane sulfonic acid, pH 7.0, 0.01 v/v % Tween-20, 0.01 m/v % BSA] supplemented with 5 μM iron(II) ammonium sulfate hexahydrate (Sigma), 3 μM α-KG (Sigma), 300 nM 21-mer biotinylated H3K4me3 peptide (GenScript), and 100 μM ascorbic acid (Fisher Scientific). The reaction was started by the addition of 30 nM $KDM5A_{1-797}$ in the assay buffer and then incubated for 40 min at room temperature. The final concentration of DMSO was 2%. The demethylation reaction was quenched by the addition of a detection mix containing 2 nM europium-conjugated anti-H3K4(me1-2) antibody (PerkinElmer), 100 nM Ulight−streptavidin conjugate (PerkinElmer), 2 mM EDTA, pH 8.0, and 1× LANCE detection buffer (PerkinElmer) in water. The quenched reaction mixture was covered and incubated for 1 h at room temperature and then analyzed using a SpectraMax M5e

https://doi.org/10.1021/acs.jmedchem.2c00725
J. Med. Chem. 2022, 65, 10554−10566

plate reader (Molecular Devices) using the TR-FRET mode with an excitation wavelength of 320 nm, emission wavelengths of 665 and 615 nm, 50 μs delay, 100 μs integration, and 100 reads per well. The signal was calculated as E665/E615. Values were plotted in GraphPad Prism and fit by nonlinear regression to calculate IC50 values.

Fluorescence Anisotropy. Changes to fluorescence anisotropy were monitored using a Tecan microplate reader equipped with excitation and emission polarizers (excitation: 485 nm, emission 535 nm) at room temperature. Reactions involving DNMT3A (or distinct DNMT3A heterotetramers) complexes with FAM-labeled DNA were carried out in the following buffer: 50 mM KH_2PO_4/K_2HPO_4 (pH 7.8), 1 mM EDTA, 1 mM DTT, 0.2 mg/mL BSA, and 20 mM NaCl with 50 μM sinefungin. The DNA substrate (Gcbox30) for binding reactions consisted of a duplex with a fluorescein (6-FAM) label on the 5′ end of the top strand (5′/6 FAM/TGGATATC-TAGGGGCGCTATGATATCT-3′; the recognition site for DNMT3A is underlined).[46] In brief, fluorescence anisotropy measurements of DNA-bound DNMT3A homo- or heterotetramers were taken following a 5 min incubation after the addition of compound 1, 2, or DMSO. Alternatively, compounds were added to DNMT3A 40 min following the addition of poly dI-dC to assess whether these compounds inhibit catalytically active DNMT3A.

Computational Docking. Using SWISS-MODEL a model of a single monomer of the catalytic domain (res 629−912) of DNMT3A was constructed using the solved crystal structure 4U7T as a template.[76] This structure was then prepared for docking using AutoDock Tools.[77] The structures of the small molecules were prepared using Gypsum-DL.[78] The small molecules were docked to the protein surface using AutoDock Vina.[77] To validate this initial setup, the native ligand SAH was docked into the active-site pocket. Its rmsd from the crystal structure is less than 2.0 A[42] (work submitted for publication).

Computational Dynamics. The docked protein−ligand complexes were evaluated using the GROMACS 2020.04 molecular dynamics software package.[79−81] The CHARMM36m force field was used to parameterize the protein structure,[82,83] and the small molecules were parameterized with the CGenFF tool.[84] The assembled complex was solvated with TIP3P water molecules and neutralized with chloride counterions. This system was subsequently minimized and simulated for 100 ps first at constant volume and temperature (*NVT*) and then at constant pressure and temperature (*NPT*). Restraints were applied to the heavy atoms in the complex during these steps. This resulted in a protein−ligand system equilibrated at 300 K. The complexes were subjected to an unrestrained 10 ns dynamics simulation, and the rmsd of the ligand with respect to the protein backbone was computed using GROMACS.

Computational Affinity Calculations. Using the trajectory file containing the positions, velocities, and forces for the atoms in the 10 ns protein−ligand simulation, molecular mechanics-generalized Born surface area (MM/GBSA) calculations were performed. This method approximates binding affinity using five distinct energy terms examining the difference between the bound and unbound forms (eq 1). These calculations were handled by the program gmx MMPBSA (63).

$$\Delta G_{\text{bind}} = (\Delta E_{\text{VdW}} + \Delta V_{\text{el}} + \Delta V_{\text{int}}) + (\Delta G_{\text{polar}} + \Delta G_{\text{non-polar}})$$

The five energy terms can be divided into two groups. The van der Waals', Coulombic, and internal energies were computed using standard MM methods, while the changes in polar and nonpolar energy were determined using the generalized Born (GB) method and changes in solvent-accessible surface area, respectively.

Cell Culture. HL60, K562, MV411, OCI-AML3, KASUMI, THP-1, and MOLM13 cells were cultured in RPMI 1460 supplemented with 10% fetal bovine serum, 5% penicillin/streptomycin, and 5% L-glutamine at 37 °C with 5% CO_2. All cell lines were obtained from ATCC and negative for mycoplasma contamination.

Flow Cytometry Analysis of AML Cells. Leukemia cell lines were seeded at 1 × 10^6 cells/mL, and various concentrations of DMSO or DNMT3A inhibitor were added. To assess differentiation, cells were harvested at 72 h and stained with markers for CD11b PE (Biolegend, cat. no. 101208, 1:100) and PI (Sigma, cat. no. P4864-10ML, 1:100). PI negative cells were selected to evaluate the differentiation status of live cells. Apoptosis levels were measured in human AML cells treated with DMSO or the DNMT3A inhibitor at indicated concentrations after staining with annexinV PE (Biolegend, cat. no. 640908). Data were analyzed using LSRII (BD) instruments.

Global Levels of 5-Methylcytosine. DNA was harvested from leukemia cell lines using Invitrogen's PureLink Genomic DNA Mini Kit (cat no. K182002) and used to quantify the global levels of 5-methylcytosine (5-mc) using Epigentek's MethylFlash Global DNA Methylation (5-mC) ELISA Easy Kit (cat no. P-1030-48). 100 ng of DNA was used, and the protocol was followed as described in the manufacturer's instructions.

■ ASSOCIATED CONTENT

Supporting Information

The Supporting Information is available free of charge at https://pubs.acs.org/doi/10.1021/acs.jmedchem.2c00725.

Substitutions to DNMT3A assessed in this study; compounds 1 and 2 not inhibiting the activity of the H3K4 histone demethylase KDM5A; molecular dynamics simulations showing that compounds 1 and 2 stably bind the tetramer interface; compound 2 increasing CD11b expression in distinct live AML cell lines; dose−response curves for a panel of 7 AML cell lines treated with increasing concentrations of compound 2; and HPLC/MS traces for compounds 1 and 2 (PDF)

Molecular formula strings (CSV)

■ AUTHOR INFORMATION

Corresponding Author

Norbert Reich − *Department of Chemistry and Biochemistry, University of California, Santa Barbara, California 93106-9510, United States;* orcid.org/0000-0001-6032-2704; Phone: (805) 893-8368; Email: reich@chem.ucsb.edu

Authors

Jonathan E. Sandoval − *Department of Chemistry and Biochemistry and Department of Molecular, Cellular and Developmental Biology, University of California, Santa Barbara, California 93106-9510, United States;* orcid.org/0000-0003-1986-0804

Raghav Ramabadran − *Stem Cells and Regenerative Medicine Center, Baylor College of Medicine, Houston, Texas 77030, United States; Department of Molecular and Cellular Biology and Interdepartmental Program in Integrative Molecular and Biomedical Sciences, Baylor College of Medicine, Houston, Texas 77030, United States*

Nathaniel Stillson − *Department of Chemistry and Biochemistry, University of California, Santa Barbara, California 93106-9510, United States*

Letitia Sarah − *Department of Cellular and Molecular Pharmacology, University of California San Francisco, San Francisco, California 94158, United States*

Danica Galonić Fujimori − *Department of Cellular and Molecular Pharmacology, University of California San Francisco, San Francisco, California 94158, United States;* orcid.org/0000-0002-4066-9417

Margaret A. Goodell − *Stem Cells and Regenerative Medicine Center, Baylor College of Medicine, Houston, Texas 77030, United States; Department of Molecular and Cellular*

Biology, Baylor College of Medicine, Houston, Texas 77030, United States

Complete contact information is available at: https://pubs.acs.org/10.1021/acs.jmedchem.2c00725

Author Contributions

The manuscript was written through contributions of all authors, and all authors have given approval to the final version of the manuscript.

Funding

This work was financially supported by the National Science Foundation (NSF) award number 1413722.

Notes

The authors declare no competing financial interest.

■ ABBREVIATIONS

CD11b, integrin subunit alpha M.; DNMTs, DNA methyltransferases; DNMT3A, DNA (cytosine-5)-methyltransferase 3A; DNMT3L, DNA-methyltransferase 3-like; DNMT1, DNA methyltransferase 1; HATs, histone acetyl transferases; HMTs, histone methyltransferases; PPIs, protein−protein interactions; p53, tumor protein P53; TDG, thymine-DNA glycosylase

■ REFERENCES

(1) Álvarez-Errico, D.; Vento-Tormo, R.; Sieweke, M.; Ballestar, E. Epigenetic Control of Myeloid Cell Differentiation, Identity and Function. *Nat Rev Immunol* **2015**, *15*, 7−17.

(2) Kiefer, J. C. Epigenetics in Development. *Dev. Dyn.* **2007**, *236*, 1144−1156.

(3) Biswas, S.; Rao, C. M. Epigenetic Tools (The Writers, The Readers and The Erasers) and Their Implications in Cancer Therapy. *Eur. J. Pharmacol.* **2018**, *837*, 8−24.

(4) Nicholson, T. B.; Veland, N.; Chen, T. Writers, Readers, and Erasers of Epigenetic Marks. In *Epigenetic Cancer Therapy*; Gray, S. G., Ed.; Academic Press: Boston, 2015, pp 31−66. DOI: 10.1016/B978-0-12-800206-3.00003-3.

(5) Ye, F.; Huang, J.; Wang, H.; Luo, C.; Zhao, K. Targeting Epigenetic Machinery: Emerging Novel Allosteric Inhibitors. *Pharmacol. Ther.* **2019**, *204*, 107406.

(6) Zucconi, B. E.; Cole, P. A. Allosteric Regulation of Epigenetic Modifying Enzymes. *Curr. Opin. Chem. Biol.* **2017**, *39*, 109−115.

(7) Bird, A. Perceptions of Epigenetics. *Nature* **2007**, *447*, 396−398.

(8) Hanna, C. W.; Kelsey, G. Features and Mechanisms of Canonical and Noncanonical Genomic Imprinting. *Genes Dev.* **2021**, *35*, 821−834.

(9) Qi, W.; Zhao, K.; Gu, J.; Huang, Y.; Wang, Y.; Zhang, H.; Zhang, M.; Zhang, J.; Yu, Z.; Li, L.; Teng, L.; Chuai, S.; Zhang, C.; Zhao, M.; Chan, H.; Chen, Z.; Fang, D.; Fei, Q.; Feng, L.; Feng, L.; Gao, Y.; Ge, H.; Ge, X.; Li, G.; Lingel, A.; Lin, Y.; Liu, Y.; Luo, F.; Shi, M.; Wang, L.; Wang, Z.; Yu, Y.; Zeng, J.; Zeng, C.; Zhang, L.; Zhang, Q.; Zhou, S.; Oyang, C.; Atadja, P.; Li, E. An Allosteric PRC2 Inhibitor Targeting the H3K27me3 Binding Pocket of EED. *Nat. Chem. Biol.* **2017**, *13*, 381−388.

(10) Siarheyeva, A.; Senisterra, G.; Allali-Hassani, A.; Dong, A.; Dobrovetsky, E.; Wasney, G. A.; Chau, I.; Marcellus, R.; Hajian, T.; Liu, F.; Korboukh, I.; Smil, D.; Bolshan, Y.; Min, J.; Wu, H.; Zeng, H.; Loppnau, P.; Poda, G.; Griffin, C.; Aman, A.; Brown, P. J.; Jin, J.; Al-awar, R.; Arrowsmith, C. H.; Schapira, M.; Vedadi, M. An Allosteric Inhibitor of Protein Arginine Methyltransferase 3. *Structure* **2012**, *20*, 1425−1435.

(11) Liu, F.; Li, F.; Ma, A.; Dobrovetsky, E.; Dong, A.; Gao, C.; Korboukh, I.; Liu, J.; Smil, D.; Brown, P. J.; Frye, S. V.; Arrowsmith, C. H.; Schapira, M.; Vedadi, M.; Jin, J. Exploiting an Allosteric Binding Site of PRMT3 Yields Potent and Selective Inhibitors. *J. Med. Chem.* **2013**, *56*, 2110−2124.

(12) Zhang, Q.; Chen, Y.; Ni, D.; Huang, Z.; Wei, J.; Feng, L.; Su, J.-C.; Wei, Y.; Ning, S.; Yang, X.; Zhao, M.; Qiu, Y.; Song, K.; Yu, Z.; Xu, J.; Li, X.; Lin, H.; Lu, S.; Zhang, J. Targeting a Cryptic Allosteric Site of SIRT6 with Small-Molecule Inhibitors That Inhibit the Migration of Pancreatic Cancer Cells. *Acta Pharm. Sin. B* **2022**, *12*. DOI: 10.1016/j.apsb.2021.06.015.

(13) Yu, J.; Xie, T.; Wang, Z.; Wang, X.; Zeng, S.; Kang, Y.; Hou, T. DNA Methyltransferases: Emerging Targets for the Discovery of Inhibitors as Potent Anticancer Drugs. *Drug Discovery Today* **2019**, *24*, 2323−2331.

(14) Santi, D. V.; Norment, A.; Garrett, C. E. Covalent Bond Formation between a DNA-Cytosine Methyltransferase and DNA Containing 5-Azacytosine. *Proc. Natl. Acad. Sci. U.S.A.* **1984**, *81*, 6993−6997.

(15) Stresemann, C.; Lyko, F. Modes of Action of the DNA Methyltransferase Inhibitors Azacytidine and Decitabine. *Int. J. Cancer* **2008**, *123*, 8−13.

(16) Siedlecki, P.; Boy, R. G.; Musch, T.; Brueckner, B.; Suhai, S.; Lyko, F.; Zielenkiewicz, P. Discovery of Two Novel, Small-Molecule Inhibitors of DNA Methylation. *J. Med. Chem.* **2006**, *49*, 678−683.

(17) Brueckner, B.; Garcia Boy, R.; Siedlecki, P.; Musch, T.; Kliem, H. C.; Zielenkiewicz, P.; Suhai, S.; Wiessler, M.; Lyko, F. Epigenetic Reactivation of Tumor Suppressor Genes by a Novel Small-Molecule Inhibitor of Human DNA Methyltransferases. *Cancer Res.* **2005**, *65*, 6305−6311.

(18) Halby, L.; Champion, C.; Sénamaud-Beaufort, C.; Ajjan, S.; Drujon, T.; Rajavelu, A.; Ceccaldi, A.; Jurkowska, R.; Lequin, O.; Nelson, W. G.; Guy, A.; Jeltsch, A.; Guianvarc'h, D.; Ferroud, C.; Arimondo, P. B. Rapid Synthesis of New DNMT Inhibitors Derivatives of Procainamide. *Chembiochem* **2012**, *13*, 157−165.

(19) Datta, J.; Ghoshal, K.; Denny, W. A.; Gamage, S. A.; Brooke, D. G.; Phiasivongsa, P.; Redkar, S.; Jacob, S. T. A New Class of Quinoline-Based DNA Hypomethylating Agents Reactivates Tumor Suppressor Genes by Blocking DNA Methyltransferase 1 Activity and Inducing Its Degradation. *Cancer Res.* **2009**, *69*, 4277−4285.

(20) Valente, S.; Liu, Y.; Schnekenburger, M.; Zwergel, C.; Cosconati, S.; Gros, C.; Tardugno, M.; Labella, D.; Florean, C.; Minden, S.; Hashimoto, H.; Chang, Y.; Zhang, X.; Kirsch, G.; Novellino, E.; Arimondo, P. B.; Miele, E.; Ferretti, E.; Gulino, A.; Diederich, M.; Cheng, X.; Mai, A. Selective Non-Nucleoside Inhibitors of Human DNA Methyltransferases Active in Cancer Including in Cancer Stem Cells. *J. Med. Chem.* **2014**, *57*, 701−713.

(21) Pappalardi, M. B.; Keenan, K.; Cockerill, M.; Kellner, W. A.; Stowell, A.; Sherk, C.; Wong, K.; Pathuri, S.; Briand, J.; Steidel, M.; Chapman, P.; Groy, A.; Wiseman, A. K.; McHugh, C. F.; Campobasso, N.; Graves, A. P.; Fairweather, E.; Werner, T.; Raoof, A.; Butlin, R. J.; Rueda, L.; Horton, J. R.; Fosbenner, D. T.; Zhang, C.; Handler, J. L.; Muliaditan, M.; Mebrahtu, M.; Jaworski, J.-P.; McNulty, D. E.; Burt, C.; Eberl, H. C.; Taylor, A. N.; Ho, T.; Merrihew, S.; Foley, S. W.; Rutkowska, A.; Li, M.; Romeril, S. P.; Goldberg, K.; Zhang, X.; Kershaw, C. S.; Bantscheff, M.; Jurewicz, A. J.; Minthorn, E.; Grandi, P.; Patel, M.; Benowitz, A. B.; Mohammad, H. P.; Gilmartin, A. G.; Prinjha, R. K.; Ogilvie, D.; Carpenter, C.; Heerding, D.; Baylin, S. B.; Jones, P. A.; Cheng, X.; King, B. W.; Luengo, J. I.; Jordan, A. M.; Waddell, I.; Kruger, R. G.; McCabe, M. T. Discovery of a First-in-Class Reversible DNMT1-Selective Inhibitor with Improved Tolerability and Efficacy in Acute Myeloid Leukemia. *Nat. Cancer* **2021**, *2*, 1002−1017.

(22) Ley, T. J.; Ding, L.; Walter, M. J.; McLellan, M. D.; Lamprecht, T.; Larson, D. E.; Kandoth, C.; Payton, J. E.; Baty, J.; Welch, J.; Harris, C. C.; Lichti, C. F.; Townsend, R. R.; Fulton, R. S.; Dooling, D. J.; Koboldt, D. C.; Schmidt, H.; Zhang, Q.; Osborne, J. R.; Lin, L.; O'Laughlin, M.; McMichael, J. F.; Delehaunty, K. D.; McGrath, S. D.; Fulton, L. A.; Magrini, V. J.; Vickery, T. L.; Hundal, J.; Cook, L. L.; Conyers, J. J.; Swift, G. W.; Reed, J. P.; Alldredge, P. A.; Wylie, T.; Walker, J.; Kalicki, J.; Watson, M. A.; Heath, S.; Shannon, W. D.; Varghese, N.; Nagarajan, R.; Westervelt, P.; Tomasson, M. H.; Link, D. C.; Graubert, T. A.; DiPersio, J. F.; Mardis, E. R.; Wilson, R. K.

DNMT3AMutations in Acute Myeloid Leukemia. *N. Engl. J. Med.* **2010**, *363*, 2424−2433.
(23) Yang, L.; Rau, R.; Goodell, M. A. DNMT3A in Haematological Malignancies. *Nat. Rev. Cancer* **2015**, *15*, 152−165.
(24) Du, J.; Johnson, L. M.; Jacobsen, S. E.; Patel, D. J. DNA Methylation Pathways and Their Crosstalk with Histone Methylation. *Nat. Rev. Mol. Cell Biol.* **2015**, *16*, 519−532.
(25) Vaissiere, T.; Sawan, C.; Herceg, Z. Epigenetic Interplay between Histone Modifications and DNA Methylation in Gene Silencing. *Mutat. Res., Rev. Mutat. Res.* **2008**, *659*, 40−48.
(26) Lian, Y.; Meng, L.; Ding, P.; Sang, M. Epigenetic Regulation of MAGE Family in Human Cancer Progression-DNA Methylation, Histone Modification, and Non-Coding RNAs. *Clin. Epigenet.* **2018**, *10*, 115.
(27) Viré, E.; Brenner, C.; Deplus, R.; Blanchon, L.; Fraga, M.; Didelot, C.; Morey, L.; Van Eynde, A.; Bernard, D.; Vanderwinden, J.-M.; Bollen, M.; Esteller, M.; Di Croce, L.; de Launoit, Y.; Fuks, F. The Polycomb Group Protein EZH2 Directly Controls DNA Methylation. *Nature* **2006**, *439*, 871−874.
(28) Mohammad, H. P.; Cai, Y.; McGarvey, K. M.; Easwaran, H.; Van Neste, L.; Ohm, J. E.; O'Hagan, H. M.; Baylin, S. B. Polycomb CBX7 Promotes Initiation of Heritable Repression of Genes Frequently Silenced with Cancer-Specific DNA Hypermethylation. *Cancer Res.* **2009**, *69*, 6322−6330.
(29) Zhao, Q.; Rank, G.; Tan, Y. T.; Li, H.; Moritz, R. L.; Simpson, R. J.; Cerruti, L.; Curtis, D. J.; Patel, D. J.; Allis, C. D.; Cunningham, J. M.; Jane, S. M. PRMT5-Mediated Methylation of Histone H4R3 Recruits DNMT3A, Coupling Histone and DNA Methylation in Gene Silencing. *Nat. Struct. Mol. Biol.* **2009**, *16*, 304−311.
(30) Cao, R.; Wang, L.; Wang, H.; Xia, L.; Erdjument-Bromage, H.; Tempst, P.; Jones, R. S.; Zhang, Y. Role of Histone H3 Lysine 27 Methylation in Polycomb-Group Silencing. *Science* **2002**, *298*, 1039−1043.
(31) Kuzmichev, A.; Nishioka, K.; Erdjument-Bromage, H.; Tempst, P.; Reinberg, D. Histone Methyltransferase Activity Associated with a Human Multiprotein Complex Containing the Enhancer of Zeste Protein. *Genes Dev.* **2002**, *16*, 2893−2905.
(32) Blackledge, N. P.; Rose, N. R.; Klose, R. J. Targeting Polycomb Systems to Regulate Gene Expression: Modifications to a Complex Story. *Nat. Rev. Mol. Cell Biol.* **2015**, *16*, 643−649.
(33) Shin, W.-H.; Kumazawa, K.; Imai, K.; Hirokawa, T.; Kihara, D. Current Challenges and Opportunities in Designing Protein-Protein Interaction Targeted Drugs. *Adv. Appl. Bioinf. Chem.* **2020**, *Volume 13*, 11−25.
(34) Lu, H.; Zhou, Q.; He, J.; Jiang, Z.; Peng, C.; Tong, R.; Shi, J. Recent advances in the development of protein-protein interactions modulators: mechanisms and clinical trials. *Signal Transduction Targeted Ther.* **2020**, *5*, 1−23.
(35) Linhares, B. M.; Grembecka, J.; Cierpicki, T. Targeting epigenetic protein-protein interactions with small-molecule inhibitors. *Future Med. Chem.* **2020**, *12*, 1305−1326.
(36) Wang, Y. A.; Kamarova, Y.; Shen, K. C.; Jiang, Z.; Hahn, M. J.; Wang, Y.; Brooks, S. C. DNA Methyltransferase-3a Interacts with P53 and Represses P53-Mediated Gene Expression. *Cancer Biol. Ther.* **2005**, *4*, 1138−1143.
(37) Li, Y.-Q.; Zhou, P.-Z.; Zheng, X.-D.; Walsh, C. P.; Xu, G.-L. Association of Dnmt3a and Thymine DNA Glycosylase Links DNA Methylation with Base-Excision Repair. *Nucleic Acids Res.* **2007**, *35*, 390−400.
(38) Kareta, M. S.; Botello, Z. M.; Ennis, J. J.; Chou, C.; Chédin, F. Reconstitution and Mechanism of the Stimulation of de Novo Methylation by Human DNMT3L. *J. Biol. Chem.* **2006**, *281*, 25893−25902.
(39) Gaidzik, V. I.; Schlenk, R. F.; Paschka, P.; Stölzle, A.; Späth, D.; Kuendgen, A.; von Lilienfeld-Toal, M.; Brugger, W.; Derigs, H. G.; Kremers, S.; Greil, R.; Raghavachar, A.; Ringhoffer, M.; Salih, H. R.; Wattad, M.; Kirchen, H. G.; Runde, V.; Heil, G.; Petzer, A. L.; Girschikofsky, M.; Heuser, M.; Kayser, S.; Goehring, G.; Teleanu, M.-V.; Schlegelberger, B.; Ganser, A.; Krauter, J.; Bullinger, L.; Döhner, H.; Döhner, K. Clinical Impact of DNMT3A Mutations in Younger Adult Patients with Acute Myeloid Leukemia: Results of the AML Study Group (AMLSG). *Blood* **2013**, *121*, 4769−4777.
(40) Huang, S.; Stillson, N. J.; Sandoval, J. E.; Yung, C.; Reich, N. O. A Novel Class of Selective Non-Nucleoside Inhibitors of Human DNA Methyltransferase 3A. *Bioorg. Med. Chem. Lett.* **2021**, *40*, 127908.
(41) Li, B.-Z.; Huang, Z.; Cui, Q.-Y.; Song, X.-H.; Du, L.; Jeltsch, A.; Chen, P.; Li, G.; Li, E.; Xu, G.-L. Histone Tails Regulate DNA Methylation by Allosterically Activating de Novo Methyltransferase. *Cell Res.* **2011**, *21*, 1172−1181.
(42) Guo, X.; Wang, L.; Li, J.; Ding, Z.; Xiao, J.; Yin, X.; He, S.; Shi, P.; Dong, L.; Li, G.; Tian, C.; Wang, J.; Cong, Y.; Xu, Y. Structural Insight into Autoinhibition and Histone H3-Induced Activation of DNMT3A. *Nature* **2015**, *517*, 640−644.
(43) Kirtana, R.; Manna, S.; Patra, S. K. Molecular Mechanisms of KDM5A in Cellular Functions: Facets during Development and Disease. *Exp. Cell Res.* **2020**, *396*, 112314.
(44) Gehling, V. S.; Bellon, S. F.; Harmange, J.-C.; LeBlanc, Y.; Poy, F.; Odate, S.; Buker, S.; Lan, F.; Arora, S.; Williamson, K. E.; Sandy, P.; Cummings, R. T.; Bailey, C. M.; Bergeron, L.; Mao, W.; Gustafson, A.; Liu, Y.; VanderPorten, E.; Audia, J. E.; Trojer, P.; Albrecht, B. K. Identification of Potent, Selective KDM5 Inhibitors. *Bioorg. Med. Chem. Lett.* **2016**, *26*, 4350−4354.
(45) Sandoval, J. E.; Reich, N. O. The R882H Substitution in the Human de Novo DNA Methyltransferase DNMT3A Disrupts Allosteric Regulation by the Tumor Supressor P53. *J. Biol. Chem.* **2019**, *294*, 18207−18219.
(46) Holz-Schietinger, C.; Matje, D. M.; Harrison, M. F.; Reich, N. O. Oligomerization of DNMT3A Controls the Mechanism of de Novo DNA Methylation. *J. Biol. Chem.* **2011**, *286*, 41479−41488.
(47) Holz-Schietinger, C.; Matje, D. M.; Reich, N. O. Mutations in DNA Methyltransferase (DNMT3A) Observed in Acute Myeloid Leukemia Patients Disrupt Processive Methylation. *J. Biol. Chem.* **2012**, *287*, 30941−30951.
(48) Sandoval, J. E.; Huang, Y.-H.; Muise, A.; Goodell, M. A.; Reich, N. O. Mutations in the DNMT3A DNA Methyltransferase in Acute Myeloid Leukemia Patients Cause Both Loss and Gain of Function and Differential Regulation by Protein Partners. *J. Biol. Chem.* **2019**, *294*, 4898−4910.
(49) Xie, T.; Yu, J.; Fu, W.; Wang, Z.; Xu, L.; Chang, S.; Wang, E.; Zhu, F.; Zeng, S.; Kang, Y.; Hou, T. Insight into the Selective Binding Mechanism of DNMT1 and DNMT3A Inhibitors: A Molecular Simulation Study. *Phys. Chem. Chem. Phys.* **2019**, *21*, 12931−12947.
(50) Newton, A. S.; Faver, J. C.; Micevic, G.; Muthusamy, V.; Kudalkar, S. N.; Bertoletti, N.; Anderson, K. S.; Bosenberg, M. W.; Jorgensen, W. L. Structure-Guided Identification of DNMT3B Inhibitors. *ACS Med. Chem. Lett.* **2020**, *11*, 971−976.
(51) Torres, P. H. M.; Sodero, A. C. R.; Jofily, P.; Silva-Jr, F. P., Jr Key Topics in Molecular Docking for Drug Design. *Int. J. Mol. Sci.* **2019**, *20*, 4574.
(52) Koya, J.; Kataoka, K.; Sato, T.; Bando, M.; Kato, Y.; Tsuruta-Kishino, T.; Kobayashi, H.; Narukawa, K.; Miyoshi, H.; Shirahige, K.; Kurokawa, M. DNMT3A R882 Mutants Interact with Polycomb Proteins to Block Haematopoietic Stem and Leukaemic Cell Differentiation. *Nat. Commun.* **2016**, *7*, 10924.
(53) Russler-Germain, D. A.; Spencer, D. H.; Young, M. A.; Lamprecht, T. L.; Miller, C. A.; Fulton, R.; Meyer, M. R.; Erdmann-Gilmore, P.; Townsend, R. R.; Wilson, R. K.; Ley, T. J. The R882H DNMT3A Mutation Associated with AML Dominantly Inhibits Wild-Type DNMT3A by Blocking Its Ability to Form Active Tetramers. *Cancer Cell* **2014**, *25*, 442−454.
(54) Brueckner, B.; Rius, M.; Markelova, M. R.; Fichtner, I.; Hals, P.-A.; Sandvold, M. L.; Lyko, F. Delivery of 5-Azacytidine to Human Cancer Cells by Elaidic Acid Esterification Increases Therapeutic Drug Efficacy. *Mol. Cancer Ther.* **2010**, *9*, 1256−1264.
(55) Gailhouste, L.; Liew, L. C.; Hatada, I.; Nakagama, H.; Ochiya, T. Epigenetic Reprogramming Using 5-Azacytidine Promotes an Anti-

Cancer Response in Pancreatic Adenocarcinoma Cells. *Cell Death Dis.* **2018**, *9*, 1−12.
(56) Kong, X. B.; Tong, W. P.; Chou, T. C. Induction of Deoxycytidine Kinase by 5-Azacytidine in an HL-60 Cell Line Resistant to Arabinosylcytosine. *Mol. Pharmacol.* **1991**, *39*, 250−257.
(57) Lo, S. K.; Lee, S.; Ramos, R. A.; Lobb, R.; Rosa, M.; Chi-Rosso, G.; Wright, S. D. Endothelial-Leukocyte Adhesion Molecule 1 Stimulates the Adhesive Activity of Leukocyte Integrin CR3 (CD11b/CD18, Mac-1, Alpha m Beta 2) on Human Neutrophils. *J. Exp. Med.* **1991**, *173*, 1493−1500.
(58) Niitsu, N.; Hayashi, Y.; Sugita, K.; Honma, Y. Sensitization by 5-aza-2′-deoxycytidine of leukaemia cells withMLLabnormalities to induction of differentiation by all-transretinoic acid and 1α,25-dihydroxyvitamin D3. *Br. J. Haematol.* **2001**, *112*, 315−326.
(59) Jeong, M.; Park, H. J.; Celik, H.; Ostrander, E. L.; Reyes, J. M.; Guzman, A.; Rodriguez, B.; Lei, Y.; Lee, Y.; Ding, L.; Guryanova, O. A.; Li, W.; Goodell, M. A.; Challen, G. A. Loss of Dnmt3a Immortalizes Hematopoietic Stem Cells In Vivo. *Cell Rep.* **2018**, *23*, 1−10.
(60) Sanchez, P. V.; Glantz, S. T.; Scotland, S.; Kasner, M. T.; Carroll, M. Induced Differentiation of Acute Myeloid Leukemia Cells by Activation of Retinoid X and Liver X Receptors. *Leukemia* **2014**, *28*, 749−760.
(61) Guryanova, O. A.; Lieu, Y. K.; Garrett-Bakelman, F. E.; Spitzer, B.; Glass, J. L.; Shank, K.; Martinez, A. B. V.; Rivera, S. A.; Durham, B. H.; Rapaport, F.; Keller, M. D.; Pandey, S.; Bastian, L.; Tovbin, D.; Weinstein, A. R.; Teruya-Feldstein, J.; Abdel-Wahab, O.; Santini, V.; Mason, C. E.; Melnick, A. M.; Mukherjee, S.; Levine, R. L. Dnmt3a Regulates Myeloproliferation and Liver-Specific Expansion of Hematopoietic Stem and Progenitor Cells. *Leukemia* **2016**, *30*, 1133−1142.
(62) Shen, L.; Kantarjian, H.; Guo, Y.; Lin, E.; Shan, J.; Huang, X.; Berry, D.; Ahmed, S.; Zhu, W.; Pierce, S.; Kondo, Y.; Oki, Y.; Jelinek, J.; Saba, H.; Estey, E.; Issa, J.-P. J. DNA Methylation Predicts Survival and Response to Therapy in Patients with Myelodysplastic Syndromes. *J. Clin. Oncol.* **2010**, *28*, 605−613.
(63) Silverman, L. R.; Holland, J. F.; Weinberg, R. S.; Alter, B. P.; Davis, R. B.; Ellison, R. R.; Demakos, E. P.; Cornell, C. J.; Carey, R. W.; Schiffer, C. Effects of Treatment with 5-Azacytidine on the in Vivo and in Vitro Hematopoiesis in Patients with Myelodysplastic Syndromes. *Leukemia* **1993**, *7 Suppl 1*, 21−29.
(64) Yun, H.; Damm, F.; Yap, D.; Schwarzer, A.; Chaturvedi, A.; Jyotsana, N.; Lubbert, M.; Bullinger, L.; Dohner, K.; Geffers, R.; Aparicio, S.; Humphries, R. K.; Ganser, A.; Heuser, M. Impact of MLL5 Expression on Decitabine Efficacy and DNA Methylation in Acute Myeloid Leukemia. *Haematologica* **2014**, *99*, 1456−1464.
(65) Navada, S. C.; Steinmann, J.; Lübbert, M.; Silverman, L. R. Clinical Development of Demethylating Agents in Hematology. *J. Clin. Invest.* **2014**, *124*, 40−46.
(66) Blaazer, A. R.; Singh, A. K.; de Heuvel, E.; Edink, E.; Orrling, K. M.; Veerman, J. J. N.; van den Bergh, T.; Jansen, C.; Balasubramaniam, E.; Mooij, W. J.; Custers, H.; Sijm, M.; Tagoe, D. N. A.; Kalejaiye, T. D.; Munday, J. C.; Tenor, H.; Matheeussen, A.; Wijtmans, M.; Siderius, M.; de Graaf, C.; Maes, L.; de Koning, H. P.; Bailey, D. S.; Sterk, G. J.; de Esch, I. J. P.; Brown, D. G.; Leurs, R.; Leurs, R. Targeting a Subpocket in Trypanosoma Brucei Phosphodiesterase B1 (TbrPDEB1) Enables the Structure-Based Discovery of Selective Inhibitors with Trypanocidal Activity. *J. Med. Chem.* **2018**, *61*, 3870−3888.
(67) Rau, R. E.; Rodriguez, B. A.; Luo, M.; Jeong, M.; Rosen, A.; Rogers, J. H.; Campbell, C. T.; Daigle, S. R.; Deng, L.; Song, Y.; Sweet, S.; Chevassut, T.; Andreeff, M.; Kornblau, S. M.; Li, W.; Goodell, M. A. DOT1L as a Therapeutic Target for the Treatment of DNMT3A-Mutant Acute Myeloid Leukemia. *Blood* **2016**, *128*, 971−981.
(68) Sutherland, M. K.; Yu, C.; Anderson, M.; Zeng, W.; van Rooijen, N.; Sievers, E. L.; Grewal, I. S.; Law, C.-L. 5-Azacytidine Enhances the Anti-Leukemic Activity of Lintuzumab (SGN-33) in Preclinical Models of Acute Myeloid Leukemia. *MAbs* **2010**, *2*, 440−448.
(69) Bruserud, Ø.; Gjertsen, B. T.; Huang, T.-s. Induction of Differentiation and Apoptosis- A Possible Strategy in the Treatment of Adult Acute Myelogenous Leukemia. *Oncol.* **2000**, *5*, 454−462.
(70) Attema, J. L.; Papathanasiou, P.; Forsberg, E. C.; Xu, J.; Smale, S. T.; Weissman, I. L. Epigenetic Characterization of Hematopoietic Stem Cell Differentiation Using MiniChIP and Bisulfite Sequencing Analysis. *Proc. Natl. Acad. Sci. U.S.A.* **2007**, *104*, 12371−12376.
(71) Purdy, M. M.; Holz-Schietinger, C.; Reich, N. O. Identification of a Second DNA Binding Site in Human DNA Methyltransferase 3A by Substrate Inhibition and Domain Deletion. *Arch. Biochem. Biophys.* **2010**, *498*, 13−22.
(72) Holz-Schietinger, C.; Reich, N. O. The Inherent Processivity of the Human de Novo Methyltransferase 3A (DNMT3A) Is Enhanced by DNMT3L. *J. Biol. Chem.* **2010**, *285*, 29091−29100.
(73) Ayed, A.; Mulder, F. A. A.; Yi, G.-S.; Lu, Y.; Kay, L. E.; Arrowsmith, C. H. Latent and Active P53 Are Identical in Conformation. *Nat. Struct. Mol. Biol.* **2001**, *8*, 756−760.
(74) Schuermann, D.; Scheidegger, S. P.; Weber, A. R.; Bjørås, M.; Leumann, C. J.; Schär, P. 3CAPS - a structural AP-site analogue as a tool to investigate DNA base excision repair. *Nucleic Acids Res.* **2016**, *44*, 2187−2198.
(75) Peterson, S. N.; Reich, N. O. GATC Flanking Sequences Regulate Dam Activity: Evidence for How Dam Specificity May Influence Pap Expression. *J. Mol. Biol.* **2006**, *355*, 459−472.
(76) Waterhouse, A.; Bertoni, M.; Bienert, S.; Studer, G.; Tauriello, G.; Gumienny, R.; Heer, F. T.; de Beer, T. A. P.; Rempfer, C.; Bordoli, L.; Lepore, R.; Schwede, T. SWISS-MODEL: Homology Modelling of Protein Structures and Complexes. *Nucleic Acids Res.* **2018**, *46*, W296−W303.
(77) Morris, G. M.; Huey, R.; Lindstrom, W.; Sanner, M. F.; Belew, R. K.; Goodsell, D. S.; Olson, A. J. AutoDock4 and AutoDockTools4: Automated docking with selective receptor flexibility. *J. Comput. Chem.* **2009**, *30*, 2785−2791.
(78) Ropp, P. J.; Spiegel, J. O.; Walker, J. L.; Green, H.; Morales, G. A.; Milliken, K. A.; Ringe, J. J.; Durrant, J. D. Gypsum-DL: An Open-Source Program for Preparing Small-Molecule Libraries for Structure-Based Virtual Screening. *J. Cheminf.* **2019**, *11*, 34.
(79) Van Der Spoel, D.; Lindahl, E.; Hess, B.; Groenhof, G.; Mark, A. E.; Berendsen, H. J. C. GROMACS: Fast, Flexible, and Free. *J. Comput. Chem.* **2005**, *26*, 1701−1718.
(80) Hess, B.; Kutzner, C.; van der Spoel, D.; Lindahl, E. GROMACS 4: Algorithms for Highly Efficient, Load-Balanced, and Scalable Molecular Simulation. *J. Chem. Theory Comput.* **2008**, *4*, 435−447.
(81) Pronk, S.; Páll, S.; Schulz, R.; Larsson, P.; Bjelkmar, P.; Apostolov, R.; Shirts, M. R.; Smith, J. C.; Kasson, P. M.; van der Spoel, D.; Hess, B.; Lindahl, E. GROMACS 4.5: A High-Throughput and Highly Parallel Open Source Molecular Simulation Toolkit. *Bioinformatics* **2013**, *29*, 845−854.
(82) Huang, J.; Rauscher, S.; Nawrocki, G.; Ran, T.; Feig, M.; de Groot, B. L.; Grubmüller, H.; MacKerell, A. D. CHARMM36m: An Improved Force Field for Folded and Intrinsically Disordered Proteins. *Nat. Methods* **2017**, *14*, 71−73.
(83) Vanommeslaeghe, K.; Hatcher, E.; Acharya, C.; Kundu, S.; Zhong, S.; Shim, J.; Darian, E.; Guvench, O.; Lopes, P.; Vorobyov, I.; Mackerell, A. D. CHARMM General Force Field: A Force Field for Drug-like Molecules Compatible with the CHARMM All-Atom Additive Biological Force Fields. *J. Comput. Chem.* **2009**, *31*, 671−690.
(84) Vanommeslaeghe, K.; Raman, E. P.; MacKerell, A. D. Automation of the CHARMM General Force Field (CGenFF) II: Assignment of Bonded Parameters and Partial Atomic Charges. *J. Chem. Inf. Model.* **2012**, *52*, 3155−3168.

https://doi.org/10.1021/acs.jmedchem.2c00725
J. Med. Chem. 2022, 65, 10554−10566